Nonlocal polymerization-driven diffusion-model-based examination of the scaling law for holographic data storage

John T. Sheridan, Michael G. Gleeson, John V. Kelly, and Feidhlim T. O'Neill

Department of Electronic and Electrical Engineering, University College of Dublin, Belfield, Dublin 4, Ireland

Received August 27, 2004

For the first time to our knowledge, a detailed theoretical basis is provided for the well-known inverse-square scaling law of holographic diffraction, which states that replay diffraction efficiency $\eta = \Gamma/M^2$, where M is the number of gratings stored and Γ is a constant system parameter. This law is shown to hold for photopolymer recording media governed by the predictions of the nonlocal polymerization-driven diffusion model. On the basis of the analysis, we (i) propose a media inverse scaling law, (ii) relate Γ to photopolymer material parameters and the hologram geometry and replay conditions, and (iii) comment on the form and validity of the diffraction efficiency inverse-square scaling law for higher-diffraction-efficiency gratings.

OCIS codes: 090.0090, 090.2900, 090.4220, 210.2860, 160.5470, 050.0050.

The well-known scaling law of holographic diffraction,[1,2] which has been observed experimentally, states that, when choosing an optimum recording schedule, the uniform replay diffraction efficiency achievable is governed by the equation

$$\eta = \frac{\Gamma}{M^2}, \tag{1}$$

where M is the (large) number of gratings (pages) stored and Γ is a constant called the system parameter. This elegant law is experimentally observed to hold for several systems.[3–6]

In 2000[7] it was proposed that hologram formation in some classes of photopolymer materials could be well described by the nonlocal polymerization-driven diffusion (NPDD) model. This model combines nonlocal material responses (caused by polymer chain growth) and a monomer diffusion process to describe material behavior during exposure. The effect of different forms of response functions[8] and nonideal kinetic effects (i.e., termination process[9] and nonlinear material response[10]) were examined. The model was applied in combination with electromagnetic theory to extract material parameters from experimental data[11] and to compare several photopolymer recording media.[12,13]

In a recent paper,[14] arguing from a clear set of physically realizable assumptions, we estimated an optimum holographic data storage schedule with the NPDD model for specific material and recording constraints. A two-harmonic analytic form of the NPDD model was used to carry out the calculations, and no time constraints were placed on the relaxation time allowed between exposures. Although the strengths (amplitudes) of each grating harmonic were shown to be equal, the diffraction efficiencies of the resulting gratings formed were not explicitly discussed, since, to do so, nonmaterial parameters, i.e., grating thickness, would have had to be identified and discussed, and that was beyond the stated objectives.

On the basis of these results,[14] we now show that the predictions of the NPDD model obey the scaling law of diffraction. We clarify and expand upon these conditions and derive a first-order expression for Γ in terms of various grating and material parameters.

In the case of a sinusoidal exposing pattern, diffraction efficiencies of thick gratings[15] can be calculated with Kogelnik's analytic expressions for index-matched on-Bragg TE-polarized replay of an unslanted uniform transmission volume grating:

$$\eta_{-1} = \sin^2\left[\frac{\pi n_1 d}{\lambda \cos(\theta_B)}\right], \tag{2}$$

or in the case of the Raman–Nath regime[15]

$$\eta_{-1} = J_1^2\left[\frac{2\pi n_1 d}{\lambda \cos(\theta_B)}\right]. \tag{3}$$

In both equations, n_1 is the grating refractive-index modulation, d is the material layer thickness, λ is the on-Bragg replay free-space wavelength, and θ_B is the on-Bragg replay angle.

If weakly scattering gratings are being examined, then, to the first order,

$$\eta_{-1} \approx \left[\frac{\pi n_1 d}{\lambda \cos(\theta_B)}\right]^2. \tag{4}$$

Significantly, this is only true for low-diffraction-efficiency gratings. For higher diffraction efficiencies we must return to Eq. (2) or (3).

In NPDD[7,14] analysis one typically assumes that n_1 is directly proportional to N_1, the amplitude of the first harmonic of the polymer concentration. Therefore $n_1 = CN_1$, where C represents the optical characteristics of the polymer material. More-accurate relationships[16] can be used if the optical properties of the material are known.

In Ref. 14 the maximum value of N_1 achievable in a photopolymer material governed by the NPDD model was determined assuming that M identical gratings were to be produced and that no time limit was placed on the recording procedure. The exposure energies and resulting grating strengths were then calculated and compared for a range of

0146-9592/05/030239-03$15.00/0

material parameters. These include D, the diffusion constant of the monomer, which is assumed constant during exposure, and dimensionless parameter $R = DK^2/F_0 = R_0/(I_0^{\gamma}\Lambda^2)$, where $K = 2\pi/\Lambda$ is the grating vector magnitude with Λ being the grating period. F_0 is the rate of polymerization, which is proportional to the amplitude of exposing intensity I_0 raised to some power γ, defining the optical nonlinearity of the material response. Parameter R_0 is independent of the exposing intensity and period. A large R_0 value (i.e., $R \sim 10$) implies that for both large exposing intensities and high spatial frequencies the material continues to record the exposing pattern with high fidelity. Conversely, a low value of R_0 (i.e., $R \sim 0.1$) results in distortions. Parameter R forms the basis of the polymerization-driven diffusion models,[7,8] which explain reciprocity failure but do not explain the reduction at high spatial frequencies of photopolymer material responses. The NPDD model explains high spatial frequency cutoff by assuming that chains initiated at a particular time and place in the medium lead to the removal of monomer at points and times nonlocal to the point of initiation. To do so, parameter $S = \exp(-K^2\sigma/2)$ is introduced, where σ is the nonlocal material response parameter and we have assumed a material with Gaussian nonlocal material spatial response functions.[7–14] When $\sigma = 0$ and $S = 1$, we speak of a local medium in which there is no chain growth away from the point of initiation. The material parameter σ becomes larger and S becomes smaller when the chains produced are longer, removing monomer at points further removed from their point of initiation. Similarly, if the spatial frequency of the recording pattern increases (Λ decreases), S decreases in size. The smaller the value of S, the more blurred the recorded grating becomes; i.e., the lower the visibility of the recorded grating and thus the lower the fidelity of the recording.

We now reexamine the N_1 values obtained for the optimum schedules in Ref. 14 for the ranges of material parameters explored. In Fig. 1 we plot the natural logarithm of these optimum values as a function of the logarithm of the number of gratings recorded. The graphs labeled A are associated with the results presented in Table 3 in Ref. 14, for which $S = 1$, $\gamma = 1$, and $R = 0.1$ and 10. Similarly we associate B with Table 5 ($S = 1$, $\gamma = 1/2$, $R = 0.1$ and 10), C with Table 4 ($S = 0.265$, $\gamma = 1$, $R = 0.1$), and D with Table 6 ($S = 0.265$, $\gamma = 1/2$, $R = 0.1$ and 10).

The result is set of almost-parallel lines all with slopes close to -1. This indicates that the grating strengths vary in an inversely proportional manner to the number of gratings; i.e., N_1 is proportional to $1/M$ for a wide range of parameter characteristics (R, S, and γ values). Thus there is a scaling law associated with the amplitude of the first harmonic of the polymer concentration, which is physically more fundamental than the inverse-square law of diffraction.

We observe that, if $M > 10$, then the optimum schedule polymer concentration amplitudes shown in Fig. 1 obey the relationship

$$N_1 \approx \tau_0(R, S, \gamma) + \frac{\tau_{-1}(R, S, \gamma)}{M}, \tag{5}$$

where the $\tau_0(R, S, \gamma)$ and $\tau_{-1}(R, S, \gamma)$ parameters represent variations arising from the particular material parameters. From the linearity of the curves in Fig. 1 it is clear that $|\tau_0(R, S, \gamma)| \ll |\tau_{-1}(R, S, \gamma)|$. Furthermore, we note that, although N_1 is always positive, it approaches zero as M becomes large. Therefore we are effectively plotting $\ln[\tau_{-1}(R, S, \gamma)] - \ln[M]$ against $\ln[M]$. Examining the set of curves labeled A–D, we estimate the corresponding values of $\tau_{-1}(R, S, \gamma)$, which are given in Table 1.

We return to our analysis. Combining expressions (4) and (5) and assuming low diffraction efficiency and that $\tau_0(R, S, \gamma)$ is small for large M values yields

$$\eta_{-1} \approx \left[\frac{\pi d}{\lambda \cos(\theta_B)} C\tau_{-1}(R, S, \gamma)\right]^2 \frac{1}{M^2}. \tag{6}$$

This has the same form as the scaling law given in Eq. (1) with

$$\Gamma = \left[\frac{\pi d C \tau_{-1}(R, S, \gamma)}{\lambda \cos(\theta_B)}\right]^2. \tag{7}$$

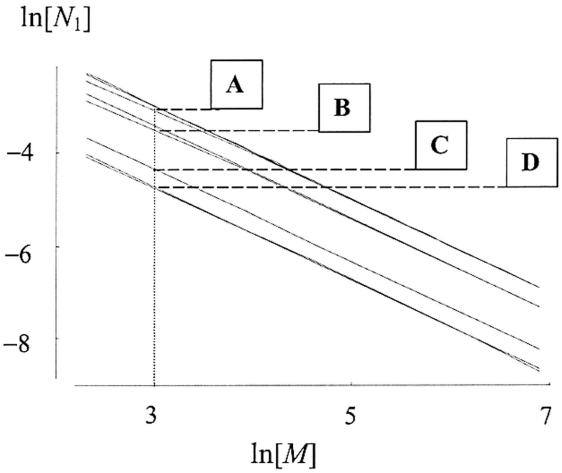

Fig. 1. $\ln(N_1)$ as a function of $\ln(M)$ for $10 < M < 1000$. The different curves (A–D) correspond to different combinations of values of R, S, and γ (see Table 1).

Table 1. NPDD based Predictions[14] of the Constant Appearing in Eq. (5)

Curve in Fig. 1	A	B	C	D
Parameters	$S = 1$, $\gamma = 1$	$S = 1$, $\gamma = 1/2$	$S = 0.265$, $\gamma = 1$	$S = 0.265$, $\gamma = 1/2$
From Ref. 14	Table 3	Table 5	Table 4	Table 6
$\tau_{-1}(R, S, \gamma)$	0.905	0.607	0.247	0.165

This equation clarifies the relationship between material and grating parameters in the scaling law. Knowing the basis of this data storage metric increases its potential for use as a first-order design tool and as a way of comparing the performance of different systems (photopolymer materials and recording geometries).

Returning to Table 1 and examining the values in light of Eq. (7), we can identify several important results. It is clear that $\tau_{-1}(R, S, \gamma)$ is largest when a local ($S = 1$), linear ($\gamma = 1$) material is used and that variations of R over the range $0.1 < R < 10$ has less effect on the value of $\tau_{-1}(R, S, \gamma)$ than the relatively small variations of S and γ. We state that, over the ranges $0.25 < S < 1$ and $0.5 < \gamma < 1$ and for $M > 10$, $\tau_{-1}(R = 0.1, S, \gamma) \approx \tau_{-1}(R = 10, S, \gamma)$. From the definitions of our parameters presented above it can be seen that variations in R caused by variations in period Λ (spatial frequency) can be compensated for by controlling exposing intensity I_0. However, as Λ decreases, S decreases and only changes in the materials chemical composition can be used to alter σ. Therefore, returning to Eq. (7), we observe that, if all the other parameters remain unchanged, then the maximum uniform diffraction efficiency possible will decrease significantly as either S or γ decreases and the material is both more nonlocal and nonlinear.

For a fixed thickness d and read–write scheme (λ, θ_B, and Λ) and assuming a fixed material composition (σ, R_0, γ), the only free parameter will be the write intensity I_0. In this case, only R can be varied, and our results imply that little manipulation of the scaling law can be achieved. However, varying I_0 will have significant effects on the duration of the exposing schedule used.[14]

These are first-order results and must be interpreted in the full context of the assumptions made in arriving at them.[14] For example, (i) the effects of nonlinear parameter γ are underestimated with the two-harmonic NPDD model, and (ii) a rigorous electromagnetic model would be required to account for the full effects of the boundaries.[17,18] Furthermore, this discussion completely neglects issues related to the signal-to-noise ratio, the bit error rate, etc. However, we believe these general trends are of practical significance.

The results presented are of general significance. The analysis provides, for the first time to our knowledge, a detailed theoretical basis for the inverse-square scale law of diffraction. Previous analysis of this issue assumed weak gratings with correspondingly low diffraction efficiencies, neglected electromagnetic efforts, i.e, Eqs. (2) and (3), and (or) assumed linear local materials.[19] We have indicated how, for storage of multiple higher-diffraction-efficiency gratings, the inverse-square law breaks down and must be replaced with Eqs. (2) and (3). Our results also indicate that an inverse material response scaling law, operating within photopolymer materials exists, e.g., expression (6). This law is clearly more fundamental than the diffraction-efficiency-based inverse-square law. Since the predictions of the NPDD model are consistent with the experimentally observed scaling law of diffraction, this provides further evidence in support of the NPDD model. Thus Eq. (7) can be used in combination with the NPDD results[14] to analyze the performance capabilities of some photopolymer-based systems. In particular, expressing Γ in terms of the τ_{-1} parameter has led us to conclusions regarding the relative significance of the material (R_0, σ, γ) and recording parameters (d, λ, θ_B). In combination with the results presented in Ref. 14, this provides several important conclusions regarding the relative suitability of photopolymer materials.

We acknowledge the support of Enterprise Ireland and Science Foundation Ireland: Research Innovation Fund and the Basic Research Grant Scheme. F. T. O'Neill holds an Irish Research Council for Science, Engineering and Technology Embark Postdoctoral Research Fellowship. J. T. Sheridan's e-mail address is john.sheridan@ucd.ie.

References

1. H. J. Coufal, D. Psaltis, and G. T. Sincerbox, eds., *Holographic Data Storage*, Springer Series in Optical Sciences (Springer-Verlag, Berlin, 2000).
2. F. H. Mok, G. W. Burr, and D. Psaltis, Opt. Lett. **21,** 896 (1996).
3. B. Pesach, E. Refaeli, and A. J. Agranat, Opt. Lett. **23,** 642 (1998).
4. M. Keskinoz and B. V. K. V. Kumar, Appl. Opt. **43,** 1368 (2004).
5. G. W. Burr, W.-C. Chou, M. A. Neifeld, H. Coufal, J. A. Hoffnagle, and C. M. Jefferson, Appl. Opt. **37,** 5431 (1998).
6. G. W. Burr, C. M. Jefferson, H. Coufal, M. Jurich, J. A. Hoffnagle, R. M. Macfarlane, and R. M. Shelby, Opt. Lett. **26,** 444 (2001).
7. J. T. Sheridan and J. R. Lawrence, J. Opt. Soc. Am. A **17,** 1108 (2000).
8. J. T. Sheridan, M. Downey, and F. T. O'Neill, J. Opt. A: Pure Appl. Opt. **3,** 477 (2001).
9. J. V. Kelly, F. T. O'Neill, and J. T. Sheridan, Proc. SPIE **5216,** 127 (2003).
10. J. R. Lawrence, F. T. O'Neill, and J. T. Sheridan, J. Opt. Soc. Am. B **19,** 621 (2002).
11. J. R. Lawrence, F. T. O'Neill, and J. T. Sheridan, J. Appl. Phys. **90,** 3142 (2001).
12. F. T. O'Neill, J. R. Lawrence, and J. T. Sheridan, Appl. Opt. **41,** 845 (2002).
13. F. T. O'Neill, J. R. Lawrence, and J. T. Sheridan, Appl. Opt. **42,** 3435 (2003).
14. J. T. Sheridan, F. T. O'Neill, and J. V. Kelly, J. Opt. Soc. Am. B **21,** 1443 (2004).
15. R. R. A. Syms, *Practical Volume Holography* (Oxford U. Press, Oxford, England, 1991).
16. I. Aubrecht, M. Miler, and I. Koudela, J. Mod. Opt. **45,** 1465 (1998).
17. S.-D. Wu and E. N. Glytsis, J. Opt. Soc. Am. A **21,** 1722 (2004).
18. S. Massenot, J.-L. Kaiser, R. Chevallier, and Y. Renotte, Appl. Opt. **43,** 5489 (2004).
19. D. Brady and D. Psaltis, J. Opt. Soc. Am. A **9,** 1167 (1992).